Mitochondrial oxidative stress and cell death in astrocytes – requirement for stored Ca^{2+} and sustained opening of the permeability transition pore

Jake Jacobson and Michael R. Duchen*

Department of Physiology, University College London, London, WC1E 6BT, UK
*Author for correspondence (e-mail: m.duchen@ucl.ac.uk)

Accepted 19 December 2001
Journal of Cell Science 115, 1175-1188 (2002) © The Company of Biologists Ltd

Summary

The role of oxidative stress is established in a range of pathologies. As mitochondria are a major source of reactive oxygen species (ROS), we have developed a model in which an intramitochondrial photosensitising agent is used to explore the consequences of mitochondrial ROS generation for mitochondrial function and cell fate in primary cells. We have found that, in astrocytes, the interplay between mitochondrial ROS and ER sequestered Ca^{2+} increased the frequency of transient mitochondrial depolarisations and caused mitochondrial Ca^{2+} loading from ER stores. The depolarisations were attributable to opening of the mitochondrial permeability transition pore (mPTP). Initially, transient events were seen in individual mitochondria, but ultimately, the mitochondrial potential ($\Delta\psi_m$) collapsed completely and irreversibly in the whole population. Both ROS and ER Ca^{2+} were required to initiate these events, but neither alone was sufficient. Remarkably, the transient events alone appeared innocuous, and caused no increase in either apoptotic or necrotic cell death. By contrast, progression to complete collapse of $\Delta\psi_m$ caused necrotic cell death. Thus increased mitochondrial ROS generation initiates a destructive cycle involving Ca^{2+} release from stores and mitochondrial Ca^{2+}-loading, which further increases ROS production. The amplification of oxidative stress and Ca^{2+} loading culminates in opening of the mPTP and necrotic cell death in primary brain cells.

Key words: Mitochondria, Oxidative stress, Permeability transition pore, Photosensitization, Intracellular calcium

Introduction

Oxidative stress plays a major role in a number of pathological states, and has been clearly established as a contributor to disease and death in ischaemia-reperfusion injury (Halestrap et al., 1998), several neurodegenerative diseases (Beal et al., 1997) and sepsis (Gutteridge and Mitchell, 1999). Moreover, the generation of reactive oxygen species (ROS) may underlie cellular changes seen in ageing (Lenaz, 1998), and ROS may act as signalling molecules in hypoxia (Duranteau et al., 1998). Mitochondria represent the major source of intracellular ROS production. Even under resting conditions between 2 and 5% of molecular oxygen consumed by mitochondria is partially reduced by the electron transport chain to form superoxide and subsequently hydrogen peroxide. Furthermore, mitochondrial ROS may inhibit one or more of the components of the respiratory chain, further accelerating the rate of superoxide formation (Turrens and Boveris, 1980). The molecular targets of mitochondrially-derived ROS have not been clearly established, although lipid peroxidation, ion channel modification and DNA damage have all been demonstrated in models where the effects of exogenous oxidising agents have been studied (Halliwell and Gutteridge, 1998)

The mitochondrial permeability transition pore (mPTP) represents a fundamental pathological process that can initiate pathways to cell death, either by causing ATP depletion and energetic collapse (Qian et al., 1999) or by promoting the release of cytochrome c and/or apoptosis-inducing factor (AIF) and precipitating apoptotic cell death (for reviews, see Bernardi et al., 1999; Crompton, 1999; Kroemer, 1999). ROS are key inducers of mPTP opening in isolated mitochondria, as oxidation of critical mitochondrial thiol groups may trigger pore opening (Crompton and Costi, 1988). In the current study, we present a model that permits the controlled generation of ROS specifically from mitochondria within cells. This allows examination of the specific consequences of mitochondrial ROS generation for both mitochondrial and cellular fate and function. Furthermore, the degree of ROS production is 'tunable' so that the consequences of different loads of radical species can be readily studied.

Several authors have described 'spontaneous', reversible mitochondrial depolarisations in cells loaded with fluorescent, potentiometric dyes. Such fluctuations of mitochondrial membrane potential ($\Delta\psi_m$) have been described in cardiomyocytes (Duchen et al., 1998; Leyssens et al., 1995; Zorov et al., 2000), neurons (Buckman and Reynolds, 2001), the COS-7 cell line (De Giorgi et al., 2000) and isolated mitochondria (Hüser et al., 1998). The depolarisations are sensitive (to varying degrees) to antioxidants, blockers of the mPTP and Ca^{2+} chelators. We have seen similar $\Delta\psi_m$ fluctuations in primary cortical astrocytes (Jacobson and Duchen, 1998) and here we have purposely used these ROS-induced depolarisations to further explore the consequences of varying degrees of mitochondrial ROS formation in astrocytes.

Our data lead us to propose a model in which mitochondrial

ROS generation promotes Ca^{2+} release from nearby ER. As this probably occurs in microdomains close to mitochondria, it results in mitochondrial calcium accumulation. This will further increase the rate of ROS production (Dykens, 1994), initiating a positive feedback cycle. In addition, the combination of michondrial calcium loading and ROS generation will increase the probability of mPTP opening, initially as transient and reversible events, but later as an irreversible state. We have then proceeded to use this approach to examine the consequences of these two states of the mPTP for cell fate. Remarkably, transient, reversible flickering of the pore appears quite innocuous and has no impact on cell fate. By contrast, once mPTP opening was sustained, necrotic cell death followed inexorably.

Materials and Methods

Preparation of adult rat cortical astrocytes

Isolated cortical astrocytes were prepared as previously described (Boitier et al., 1999; Peuchen et al., 1997). Briefly, cerebra taken from adult Sprague-Dawley rats, were transferred to EBSS, chopped and triturated until homogeneous. This suspension was passed through a 297 μm mesh (Sigma), resuspended in EBSS and washed by centrifugation. The resulting pellet of tissue was suspended in a nominally Ca^{2+}- and Mg^{2+}-free EBSS solution containing 50,000 Uml^{-1} trypsin (Type III, porcine pancreas, Sigma ref. T-7418), 336 Uml^{-1} DNAse 1 (Type IV, bovine pancreas, Sigma ref. D-5025), and collagenase 1.033 Uml^{-1} (Type XI, Sigma ref. C-9407) and placed in an incubator (36°C, 95% air, 5% CO_2). The enzymatic digestion was stopped after 15 minutes by addition of fetal calf serum (10% of final volume) and the suspension filtered through a 140 μm mesh, resuspended and centrifuged once more. The pellet was resuspended in EBSS, layered onto 0.4 M sucrose (molecular biology grade, BDH Chemicals) in EBSS and centrifuged at 400 ***g*** for 10 minutes. The resulting pellet was washed, suspended in pre-warmed D-valine MEM supplemented with 5% fetal calf serum, 2 mM glutamine and 1 mM malate and transferred to tissue culture flasks pre-coated with 0.01% poly-D-lysine. The D-valine inhibits the growth of fibroblasts. After 6 days in culture the D-val-containing medium was replaced by MEM supplemented with L-valine.

Dye loading and drug application

All solutions were based on a saline that comprised 156 mM NaCl; 3 mM KCl; 2 mM $MgSO_4$; 1.25 mM KH_2PO_4; 2 mM $CaCl_2$; 10 mM D-glucose; 10 mM Hepes; pH adjusted to 7.35. Cells were loaded with TMRE (1.5 μM) for 15 minutes at room temperature followed by washing. Cells were loaded with rhod-2 as the AM ester (4.4 μM) for 30 minutes before washing (Boitier et al., 1999). Short-acting drugs (e.g. FCCP, rotenone) were applied locally close to cells from pressurised micropipettes. In some cases (e.g. as with BAPTA-AM and antioxidants) drugs were added to the bathing saline.

Drugs and dyes

Fluorescent dyes were purchased from Molecular Probes Europe BV (Leiden, The Netherlands). N-methyl 4-valine cyclosporin was the gift of Novartis Pharma AG (Basel, Switzerland) and all other chemicals were purchased from Sigma (Poole, UK).

Imaging

Digital imaging of cells loaded with TMRE, Fura-2 or rhod-2 was performed using either a cooled CCD camera (Hamamatsu 4880) or a Zeiss 510 CLSM confocal microscope equipped with ×40 and ×63 oil immersion, quartz objective lenses (NA 1.3 and 1.4, respectively) as well as a ×40 long working distance lens (NA 0.68). For the cooled CCD system, coverslips were placed in a homemade chamber mounted on the stage and fluorescence excited using a 75 W xenon arc lamp, the light from which passed through a 546 nm band pass filter and then a 580 nm dichroic mirror. Light longer than 590 nm was collected and focussed on the camera. Fura-2 was sequentially excited at 340 nm and 380 nm and the fluorescence beyond 530 nm was imaged. On the confocal system, cells were illuminated using the 543 nm emission line of a HeNe laser and the intensity of the incident light was maintained between 0.5 and 5% of the total laser output. The fluorescence of TMRE or rhod-2 was collected at wavelengths longer than 585 nm.

To image NADH autofluorescence, cells were illuminated using the 351 nm laser line of the Zeiss 510 CLSM, and the fluorescence signal was collected through a bandpass filter between 375 and 488 nm. In order to avoid any crosstalk in cells co-loaded with TMRM, 'multitracking' was used, in which images at each optical configuration are collected successively, rather than simultaneously, on two channels. The pinhole was opened to a confocal thickness of about 5 μm to optimise light collection for the autofluorescence signal.

Image processing and statistical analysis

The incidence of mitochondrial depolarisations was assessed as follows: background-subtracted images were differentiated in time using image analysis software (Lucida 5.0, Kinetic Imaging, Liverpool, UK), emphasising only those pixels that had changed since the preceding frame (Fig. 3B). Mitochondrial depolarisations were revealed as localised, bright areas in a dark background, whereas mitochondria with a stable $\Delta\psi_m$ were not discernible and mitochondrial movement caused only small changes in signal. The peak digital value over individual cells was plotted for each frame of the differentiated image series and after normalisation to a baseline, the area under each plot was calculated (Microcal Origin 4.1 software, Northampton, MA). Hence a high frequency of mitochondrial depolarisations produced a higher integrated value than seen in quiescent cells (Fig. 5B).This value was consistent with the subjective observation of 'active' and 'quiescent' cells. In cells where the fluorescent flickers summated rapidly to produce a steadily rising global signal, the fluorescence was measured over the whole cell (omitting the mitochondrion-free nucleus) and the rate of rise was measured by fitting a line to the steepest part of the plot. Results, either the integrated values or the slopes of the fitted lines, were statistically compared using GraphPad Instat 4.00 software (San Diego, CA); data with a homogenous variance were assessed by non-paired two-tailed Student's *t*-test, those with a heterogeneous variance were assessed by Mann-Whitney U test. All data are presented as mean±standard deviation (s.d.) and the point of minimum acceptable statistical significance was taken to be 0.05.

To represent changing intensities in both space and time, we have presented data from image sequences as surface plots derived from line images. Each line of the line image displays the colour-coded fluorescence intensity profile along a line drawn through the length of the cell for one frame of an image sequence. Plotting all the lines together in temporal sequence produces a 2D image where the fluorescence values along the line are represented against time. The surface plots shown in this paper were constructed as follows: images were background-subtracted and divided by a digitally constructed 'darkest image' to represent baseline values (Duchen et al., 1998). A line was drawn along the axis of a cell and the pixel values along the line for the full image sequence were then read using Lucida software. The resultant data were imported into MatLab software (The Mathworks, Natick, MA) the ASCII matrices were used to create the surface plots shown. The colour-coded look-up table applied runs

through the spectrum, with blue representing the lowest ratio value and red the highest.

Results

TMRE fluorescence as a measure of changing $\Delta\psi_m$

Digital imaging of TMRE-loaded astrocytes clearly revealed fine intracellular structures throughout the cells. The identity of these structures as mitochondria was confirmed by colocalisation with NADH autofluorescence (Fig. 1A,B), chosen as a marker completely independent of the properties of any exogenous indicator.

When concentrated, TMRE exhibits autoquenching, such that the fluorescence signal becomes a nonlinear function of dye concentration (Bunting et al., 1989; Duchen, 1992; Duchen and Biscoe, 1992); mitochondrial depolarisation causes loss of mitochondrial dye, and dilution into the cytosol where the signal therefore increases. The TMRE fluorescence changed systematically in response to biochemical agents as predicted from chemiosmotic principles, increasing with manipulations expected to cause mitochondrial depolarisation. Thus, application of the uncoupler FCCP (1 μM), which collapses $\Delta\psi_m$, caused a brisk increase of fluorescence while the definition of mitochondrial structures was lost (Fig. 1Cii,D). Similar changes were seen in response to inhibition of mitochondrial respiration with rotenone (Fig. 1E). The images shown as Fig. 1Ciii and iv were obtained by dividing the image sequence by the first image of the sequence (Fig. 1Ci) so that the signal is normalised for each pixel. After mitochondrial depolarisation, the signal over the cytosol increased, whereas that over mitochondria had changed little so that the mitochondria appear dark against a bright cytosol. This process emphasises the proportional change in TMRE signal over each intracellular compartment.

Transient mitochondrial depolarisations in quiescent cells

When collecting imaging series with time, brief flashes of increased fluorescence were frequently seen over individual mitochondria reflecting transient mitochondrial depolarisations. Fig. 2A shows the time course of these depolarisations of individual mitochondria. Fig. 2C and D were extracted from the same image sequence, emphasising that the depolarisations were independent in time and space. Analysis of the time course of 91 mitochondrial transient depolarisations in 58 cells showed a mean time from baseline to peak fluorescence of 257.5±153.5 mseconds (mean±s.d.).

Single mitochondria could depolarise repeatedly (Fig. 2B,C). The signal over individual organelles often returned to (or even below) baseline implying that the recovery of potential could be complete. The mean signal rise was only 39±17% of that seen following complete dissipation of $\Delta\psi_m$ by FCCP (n=100, Fig. 2E). That the signal change induced by the transient depolarisations was much smaller than that seen on complete dissipation with FCCP argues that the transient depolarisations either reflect only small changes in $\Delta\psi_m$ or that they are so brief that the dye does not have time to re-equilibrate. In some cells, the transient depolarisations were overwhelmed by an increase in signal over the whole cell, although transient depolarisations of individual mitochondria were evident in the initial images. Because TMRE diffuses out of depolarised mitochondria but is retained in the short term within the cell by the plasma membrane potential (Nicholls and Ward, 2000), the global signal rise reflected the depolarisations of many mitochondria and accumulation of dye within the cytosol. Thus, the rate of rise of whole-cell fluorescence reflected the number, or magnitude, of multiple mitochondrial depolarisations. Application of FCCP (1 μM) to cells in which the fluorescence had reached a plateau failed to evoke any further signal (Fig. 2F), suggesting that the mitochondrial depolarisation was global and complete.

The sequential subtraction of successive images from an image series was used to highlight only those pixels in which the signal had changed between image frames (Fig. 3B). This process revealed ‘puffs’ of fluorescence around individual mitochondria, consistent with local loss of dye from the organelles, and emphasises that changes in TMRE signal are due to fluorophore redistribution rather than mitochondrial movement.

The frequency of transients and the rate of global depolarisation were dependent on illumination intensity

Operationally, it rapidly became apparent that the incidence of mitochondrial depolarisations was related to the intensity of illumination. Thus, reduction of the excitation light intensity significantly increased the time taken to establish global mitochondrial depolarisation (Fig. 4A). Systematically decreasing the intensity of illumination by using a range of neutral density filters significantly increased the time taken for the TMRE signal to reach an FCCP-insensitive plateau (P<0.0001, Kruskal-Wallis non-parametric ANOVA test, Fig. 4B). Three neutral density filters were used, giving 1% transmission (46 cells), 3.5% transmission (27 cells) and 5% transmission (38 cells) of excitation light. When all but 1% of the excitation light was excluded, individual mitochondria depolarised occasionally, but the global signal remained stable (Fig. 4A).

Thus the frequency of the mitochondrial depolarisations and the time to global mitochondrial depolarisation could be controlled by varying the illumination intensity. Minimising the excitation light allowed mitochondria to be observed repeatedly depolarising and repolarising with a minimal change in overall fluorescence, permitting us to explore the nature of the depolarisations and their consequences for cell function more fully.

Focal mitochondrial depolarisations were independent of external Ca^{2+}, but dependent on stored Ca^{2+}

In a previous paper (Duchen et al., 1998), we described similar mitochondrial depolarisations in single rat cardiomyocytes that were dependent upon ryanodine-sensitive sarcoplasmic reticulum Ca^{2+}-release and subsequent mitochondrial Ca^{2+}-uptake. We therefore investigated the Ca^{2+}-dependence of the depolarisations in astrocytes in which Ca^{2+} stores are largely inositol (1,4,5)-trisphosphate [Ins(1,4,5)P_3]-dependent (Boitier et al., 1999; Langley and Pearce, 1994; Peuchen et al., 1996). The mitochondrial depolarisations were unaffected by removal of extracellular Ca^{2+}. In the presence of a Ca^{2+}-free saline containing 1 mM EGTA the integrated activity (see

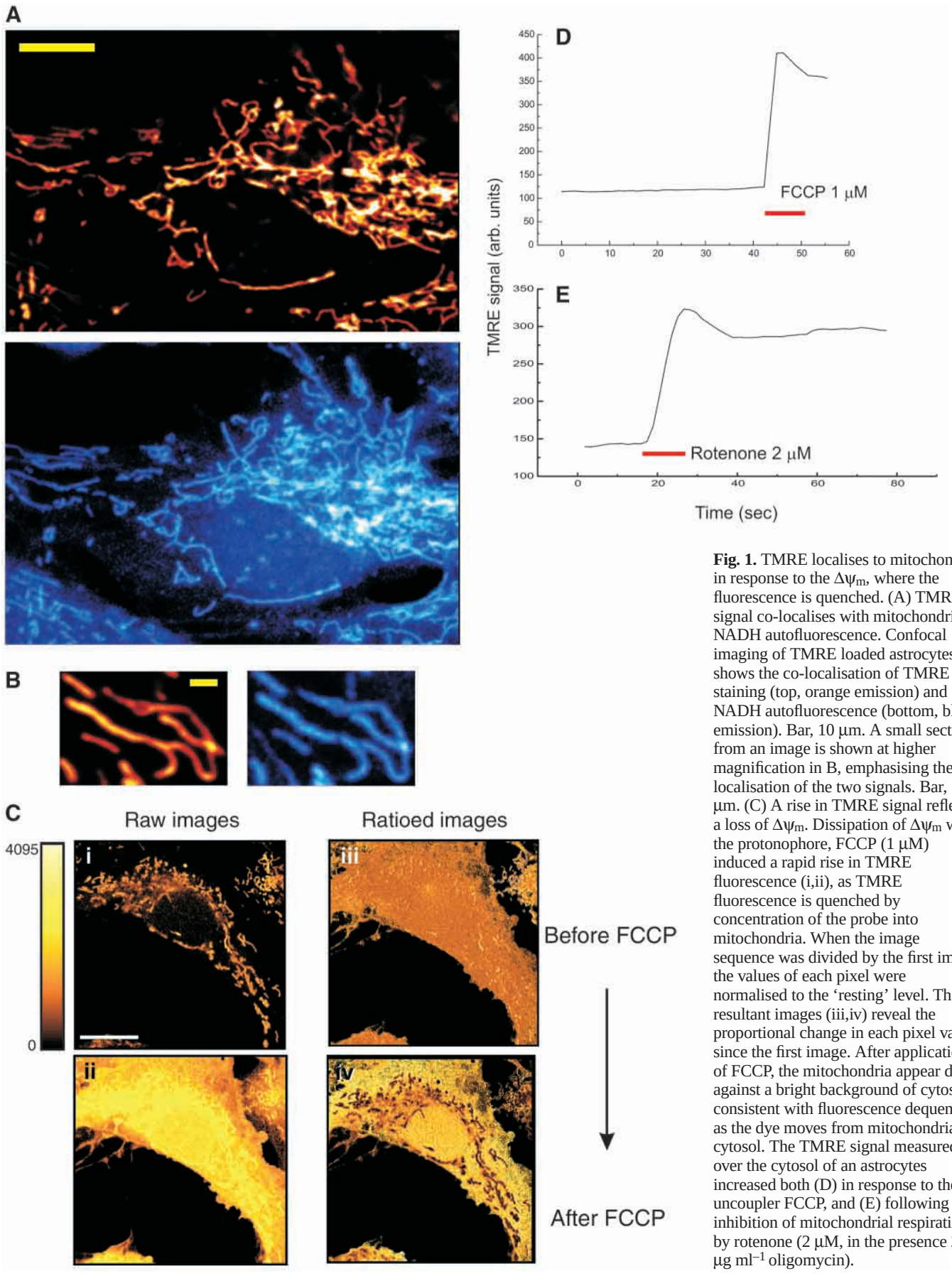

Fig. 1. TMRE localises to mitochondria in response to the $\Delta\psi_m$, where the fluorescence is quenched. (A) TMRE signal co-localises with mitochondrial NADH autofluorescence. Confocal imaging of TMRE loaded astrocytes shows the co-localisation of TMRE staining (top, orange emission) and NADH autofluorescence (bottom, blue emission). Bar, 10 μm. A small section from an image is shown at higher magnification in B, emphasising the co-localisation of the two signals. Bar, 1 μm. (C) A rise in TMRE signal reflects a loss of $\Delta\psi_m$. Dissipation of $\Delta\psi_m$ with the protonophore, FCCP (1 μM) induced a rapid rise in TMRE fluorescence (i,ii), as TMRE fluorescence is quenched by concentration of the probe into mitochondria. When the image sequence was divided by the first image, the values of each pixel were normalised to the 'resting' level. The resultant images (iii,iv) reveal the proportional change in each pixel value since the first image. After application of FCCP, the mitochondria appear dark against a bright background of cytosol, consistent with fluorescence dequench as the dye moves from mitochondria to cytosol. The TMRE signal measured over the cytosol of an astrocytes increased both (D) in response to the uncoupler FCCP, and (E) following inhibition of mitochondrial respiration by rotenone (2 μM, in the presence 2.5 μg ml^{-1} oligomycin).

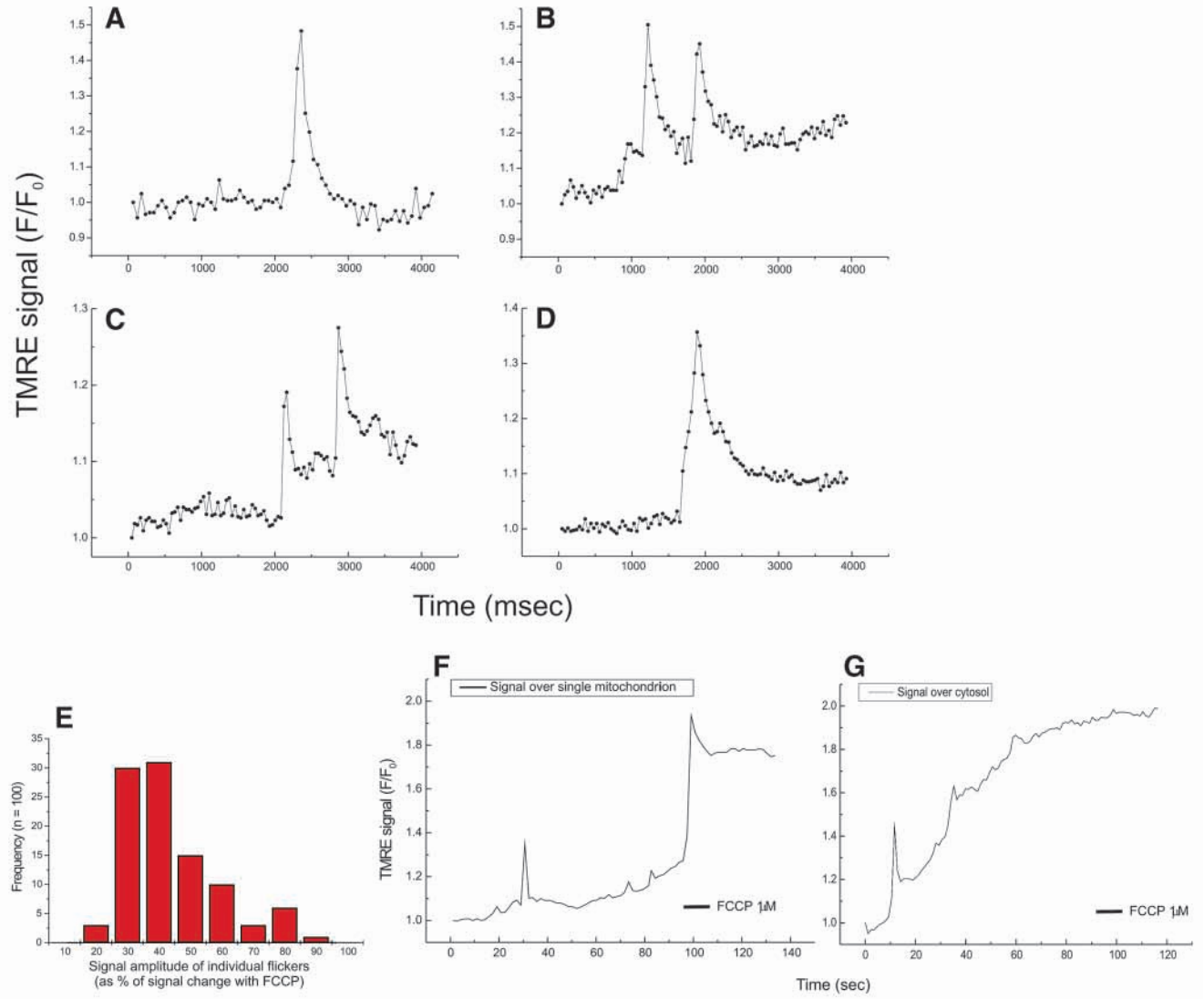

Fig. 2. Imaging of TMRE-loaded astrocytes revealed transient fluctuations in $\Delta\psi_m$. (A-D) Imaging of TMRE-loaded cells revealed brief, spontaneous and reversible depolarisations of individual mitochondria. The fluorescence signal over individual mitochondria is plotted as a function of time. Note that the signal over individual organelles frequently returned to baseline, suggesting complete mitochondrial repolarisation following a depolarisation (A) and single organelles could depolarise and repolarise repeatedly (B,C), further suggesting reversible depolarisations of $\Delta\psi_m$. The traces in C and D were obtained from two mitochondria in a single cell, demonstrating that the flickers were independent in time and did not reflect a global loss of $\Delta\psi_m$. The histogram in E, shows the distribution of the relative amplitudes of individual transient changes in signal. FCCP was applied at the end of each imaging sequence, and the amplitudes are expressed as a percentage of the response to FCCP. In some cells the global fluorescence was essentially stable, so that individual depolarisations were easily discernible (F), and were much smaller in amplitude than the response to FCCP. In other cells, the flickers rapidly summated to produce a global rise in whole-cell fluorescence that overwhelmed the signal produced by individual mitochondria (G), in which case application of FCCP induced no further change in signal, suggesting that mitochondrial depolarisation was complete.

Image processing and statistical analysis) was 13.7±2.4 (n=19), compared with matched controls of 13.2±3.2 (n=10) (P=0.703, Mann-Whitney U test). To investigate the role of intracellular Ca^{2+}, the cells were loaded with the membrane-permeant Ca^{2+} chelator, BAPTA-AM (10 μM). Again this had no impact on the transient depolarisations (the integrated activity of the BAPTA-treated group was 11.8±2.7 with controls of 12.2±4.2, (n=21; P=0.7, Mann-Whitney U test). These data could suggest that the events are independent of $[Ca^{2+}]_{cyt}$. However, in some cell types, recent data suggest a privileged access of ER Ca^{2+} to mitochondria (Rizzuto et al., 1998), and if applicable to cortical astrocytes might explain mitochondrial Ca^{2+}-accumulation insensitive to BAPTA.

Mitochondrial Ca^{2+}-uptake may be blocked by ruthenium red, but this is membrane impermeant, not very selective, and interferes with TMRE fluorescence (e.g. Chamberlain et al., 1984) (M.R.D., unpublished). We therefore tested a derivative of ruthenium red, Ru-360, which blocks mitochondrial Ca^{2+}-uptake in cardiomyocytes (Matlib et al., 1998). Unfortunately, in our hands this agent induced depletion of Ca^{2+} stores in the astrocytes (data not shown), and so could not be used.

Intracellular Ca^{2+} stores can be depleted by inhibition of the

sarcoplasmic/endoplasmic reticulum Ca^{2+} ATPase (SERCA) with thapsigargin. However, thapsigargin may induce mitochondrial Ca^{2+}-loading (Ricken et al., 1998; Sheu and Sharma, 1999), and so sensitise the mitochondria to ROS production. We therefore loaded cells with BAPTA-AM before exposure to thapsigargin (200 nM), in order to chelate Ca^{2+} released from the ER by thapsigargin and so limit mitochondrial Ca^{2+}-loading. The BAPTA loading prevented any rise in $[Ca^{2+}]_{cyt}$ in response to thapsigargin – the resting fura-2 ratio was unchanged in treated cells compared with controls (P=0.540, unpaired t-test, n=6). The efficient and complete emptying of stores by the manoeuvre was confirmed as the response to ATP, a Ca^{2+} mobilising agonist was abolished (Fig. 5A). This protocol greatly suppressed the transient events, giving an integrated activity of 10.7±2.4 (n=117; P<0.0001, Mann-Whitney U test), significantly reduced from the matched controls (14.6±5.4, n=68; Fig. 5B). Thus, ER Ca^{2+} was required for the transient mitochondrial depolarisations in cells with predominantly Ins(1,4,5)P_3-sensitive Ca^{2+} stores, illustrated further by the surface plot in Fig. 5C.

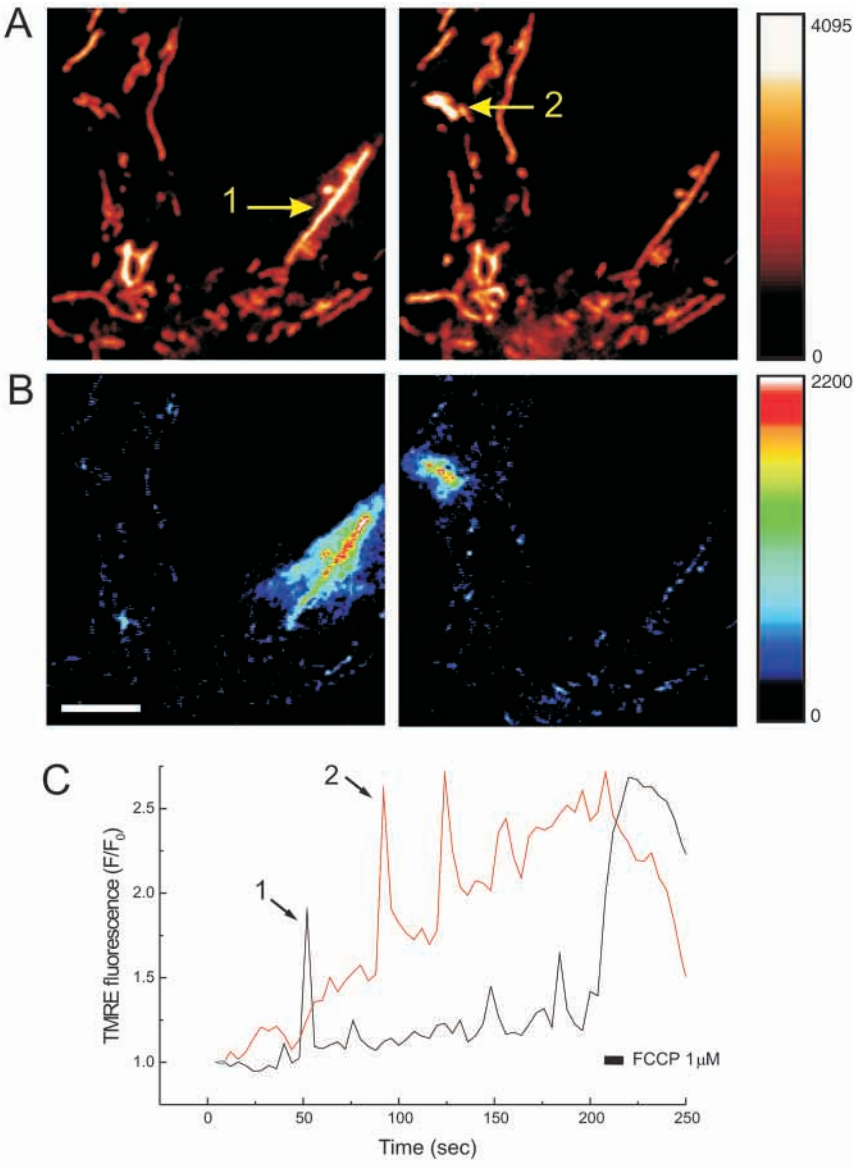

Fig. 3. Differentiation of confocal images revealed dye egress from depolarising mitochondria. (A) High magnification images (×63 oil-immersion objective), revealed depolarisations of individual mitochondria (arrows). (B) Differentiated images reveal only those pixels in which the signal changed between successive image frames. 'Clouds' of fluorescence can be seen surrounding individual mitochondria as the TMRE moves into the cytosol. Plots of the signal with time from 3A are shown in C. Arrows indicate the depolarisations illustrated in the preceding images. Bar, 5 μm.

The depolarisations reflect transient openings of the mitochondrial permeability transition pore

Uptake of Ca^{2+} by mitochondria is electrogenic and results in a reversible depolarisation of $\Delta\psi_m$ (e.g. Duchen, 1992). Ca^{2+}-dependent mitochondrial depolarisations may therefore result from the electrogenic uptake of Ca^{2+} by mitochondria in response to local Ca^{2+} transients. Alternatively, mitochondrial Ca^{2+} accumulation could promote opening of the mPTP, particularly if mitochondria are also sensitised by oxidative stress (Hüser et al., 1998). We therefore asked whether the depolarisations reflect opening of the mPTP. Cyclosporin A, the classical inhibitor of mPTP opening (Crompton et al., 1988) significantly reduced the rate of progression of the global mitochondrial depolarisation (slope of onset of TMRE dequench in controls was 0.058±0.031, n=15; in 500 nM CsA-treated, 0.004±0.005, n=17. P<0.0001, unpaired Mann-Whitney U test). Cyclosporin A binds all cyclophilins and so is not selective for the mPTP. We therefore also used N-methyl 4-valine cyclosporin (meth-v-Cs), a non-immunosuppressive analogue of cyclosporin A. Meth-v-Cs also binds cyclophilins, but the cyclophilin A/meth-v-Cs complex does not bind Ca^{2+}-sensitive calcineurin (Petronilli et al., 1994b). 400 nM meth-v-Cs significantly reduced the integrated activity (Fig. 6A) to 9.8±2.5, n=122, compared with a matched control of 12.0±2.6, n=82 (P<0.0001, two-tailed, unpaired t-test). Trifluoperazine (10 μM), another inhibitor of pore formation (Lemasters et al., 1998; Bernardi et al., 1993) also reduced the rate of global depolarisation (Fig. 6B) to a slope of 0.008±0.006 (n=60 cells; P<0.0001), compared with 0.041±0.018 (n=27) cells for the matched controls (Mann-Whitney U test). Thus, the concordance of data strongly suggests that the transient, Ca^{2+}-dependent mitochondrial depolarisations signalled reversible openings of the mPTP.

mPTP openings were suppressed by antioxidants

Illumination of fluorophores causes production of ROS. Indeed, photobleaching of fluorophores is largely an oxidative reaction and commercially available 'antifade' compounds are in fact cocktails of antioxidants. Several mitochondrial probes,

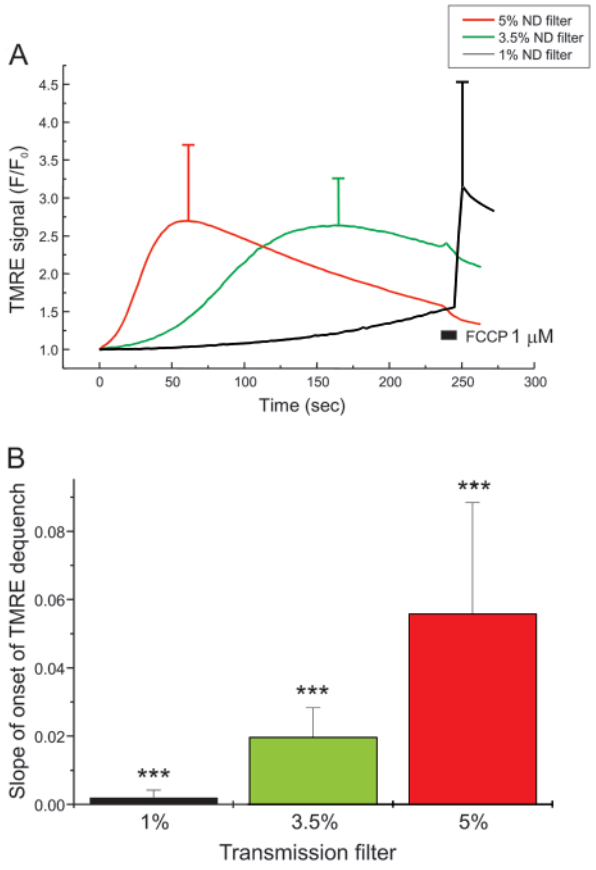

Fig. 4. Attenuation of illumination intensity increased the time to global depolarisation. (A,B) The rate of mitochondrial depolarisation was systematically slowed by attenuation of the illumination intensity by neutral density filters suggesting that ROS formation by fluorophore illumination was sensitising mPTP formation (P<0001, Kruskal-Wallis non-parametric ANOVA test, n=46, 27 and 38 cells imaged using 1%, 3.5% and 5% transmission filters, respectively).

including TMRE, produce singlet oxygen upon illumination (Bunting, 1992). As mPTP opening is induced by oxidative stress we explored the effects of a range of antioxidants on the events. Exposure of cells to a solution of ascorbic acid (1 mM), catalase (250 units ml^{-1}), the α-tocopherol analogue Trolox (1 mM) and the spin trap TEMPO (500 μM) markedly reduced the flickering depolarisations (Fig. 7A) with a reduction in integrated activity to 6.4±1.9 (n=57) from a matched control of 10.0±5.6 (n=53, P<0.001, Mann-Whitney U test). Similarly, the time taken to global depolarisation in antioxidant-treated cells was significantly prolonged (Fig. 7B) – the slope of the onset of the TMRE signal in controls was 0.094±0.034, (n=9) and in the antioxidant-treated cells, 0.002±0.003 (n=12), P<0.0001, Mann-Whitney U test.

Mitochondrial oxidative stress causes mitochondrial calcium loading

We have noticed, when using the mitochondrial Ca^{2+}-sensitive indicator rhod-2 AM, that the mitochondrial signal tends to become brighter with time, even in unstimulated cells (Fig. 8A,B), unless the illumination intensity is kept to a minimum. As fluorophores are more likely to bleach with illumination, we wondered whether ROS could be sensitising Ca^{2+}-release from intracellular stores causing mitochondrial Ca^{2+} loading. We therefore loaded astrocytes with rhod-2 AM and examined the effects of antioxidants (as used above) on the rate of signal rise with illumination. Over a period of illumination, the rhod-2 signal rose initially over the whole cell, during which the mitochondria were visible as bright organelles. The cytosolic and nuclear signals then slowly decreased, leaving bright, Ca^{2+}-loaded mitochondria. These observations were reminiscent of the rhod-2 signal changes seen when astrocytes are stimulated with ATP, an agonist of Ins(1,4,5)P_3-mediated Ca^{2+} release (Boitier et al., 1999). The mean rate of rise of the cytosolic/mitochondrial rhod-2 signal was 0.011±0.006 arbitrary units/millisecond (n=63). However, the antioxidants significantly slowed the rate of rise to 0.002±0.001 arbitrary units/millisecond (n=62; P<0.0001, Mann-Whitney U test). Thus, illumination of cells loaded with a Ca^{2+}-sensitive fluorophore induced a mitochondrial Ca^{2+}-loading that was ROS-dependent.

Transient mPTP opening is innocuous; global mitochondrial depolarisation causes necrotic cell death

We used the ability to induce mPTP opening in single astrocytes to investigate whether transient openings of the pore induced cell death. Cells were stained with propidium iodide (PI) and Hoechst 33342 to differentiate between apoptotic and necrotic endpoints. Cells were plated onto coverslips to which an etched grid (‘CELLocate’, Eppendorf) was attached. Cells could then be relocated by the grid reference hours after illumination and examined for morphological and staining changes. Conditions were established to generate only transient depolarisations (using a 1% transmission neutral density filter), keeping the global depolarisation to a minimum. The cells were then returned to culture medium and replaced in an incubator (36°C, 5% CO_2) and examined again 4 hours later using PI (10 μM) and Hoechst 33342 (15 μM). Nuclei that stained brightly with Hoechst 33342 showing chromatin condensation were scored as apoptotic if they excluded PI, while those nuclei that showed PI staining were deemed necrotic (Fig. 9A). In a further series of experiments, cells were illuminated using a 30% neutral density filter to induce a global mitochondrial depolarisation. Again, non-illuminated areas of the same dish were compared with the imaged cells 4 hours later.

In those cells in which frequent transient depolarisations had been documented without global depolarisation, no significant increase in cell death, apoptotic or necrotic, was detectable above the control levels (Fig. 9B). Of 2083 illuminated cells, only 10% displayed necrotic staining or morphology after 4 hours, while only four cells displayed apoptotic staining or morphology, compared with non-illuminated controls in which 12% of 1826 cells counted were necrotic and only three were apoptotic (P=0.962, unpaired t-test). By contrast, after sufficient illumination to induce a global mitochondrial depolarisation the incidence of necrotic cell death increased significantly after 4 hours to 35% (of 718 cells) compared with 1% of controls (of 983 counted, P=0.0002, unpaired t-test). In these cells, no apoptotic cells

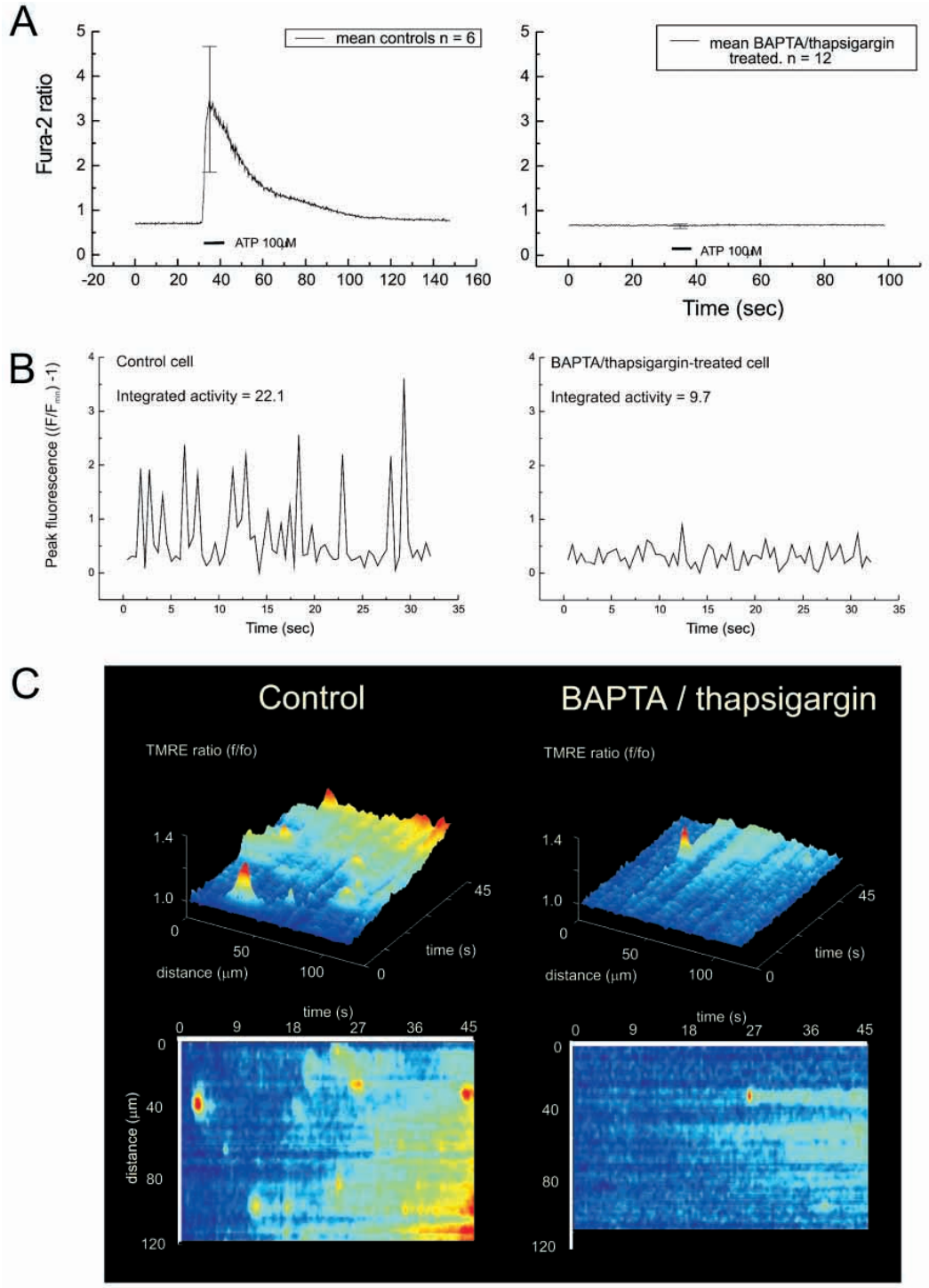

Fig. 5. Stored calcium was necessary for the mitochondrial depolarisations. (A) Astrocytes were exposed to a combination of 10 μM BAPTA-AM and 200 nM thapsigargin in order to empty intracellular Ca^{2+} stores and to chelate released Ca^{2+}. The efficacy of this manipulation was demonstrated by application of 100 μM ATP, which mediates Ins(1,4,5)P_3-mediated Ca^{2+} release (left), failed to raise $[Ca^{2+}]_c$ in the treated cells (right). (B) The relative occurrence of mitochondrial depolarisations was assayed by calculation of 'integrated activity'; digital images of each cell were differentiated, revealing how the signal changed with time. The peak signals in the differentiated series were then plotted against time and integrated in order to measure the number or amplitude of depolarisations (see Image processing and statistical analysis). The peak fluorescence with time over representative single cells is shown. Emptying and chelation of ER Ca^{2+} stores significantly reduced integrated activity: 14.6±5.4 (n=117 cells) versus 10.7±2.4 (n=68) (mean±s.d., P<0.0001, Mann-Whitney U test), confirming that stored Ca^{2+} was necessary for the mitochondrial depolarisations. Line images extracted from TMRE-loaded cells are shown in C. Treatment of cells with thapsigargin and BAPTA-AM effectively emptied ER Ca^{2+} stores. Cells were then loaded with TMRE and imaged as before. Multiple transient mitochondrial depolarisations were revealed along a line drawn through a single control cell, but very few were seen in cells treated with thapsigargin and BAPTA.

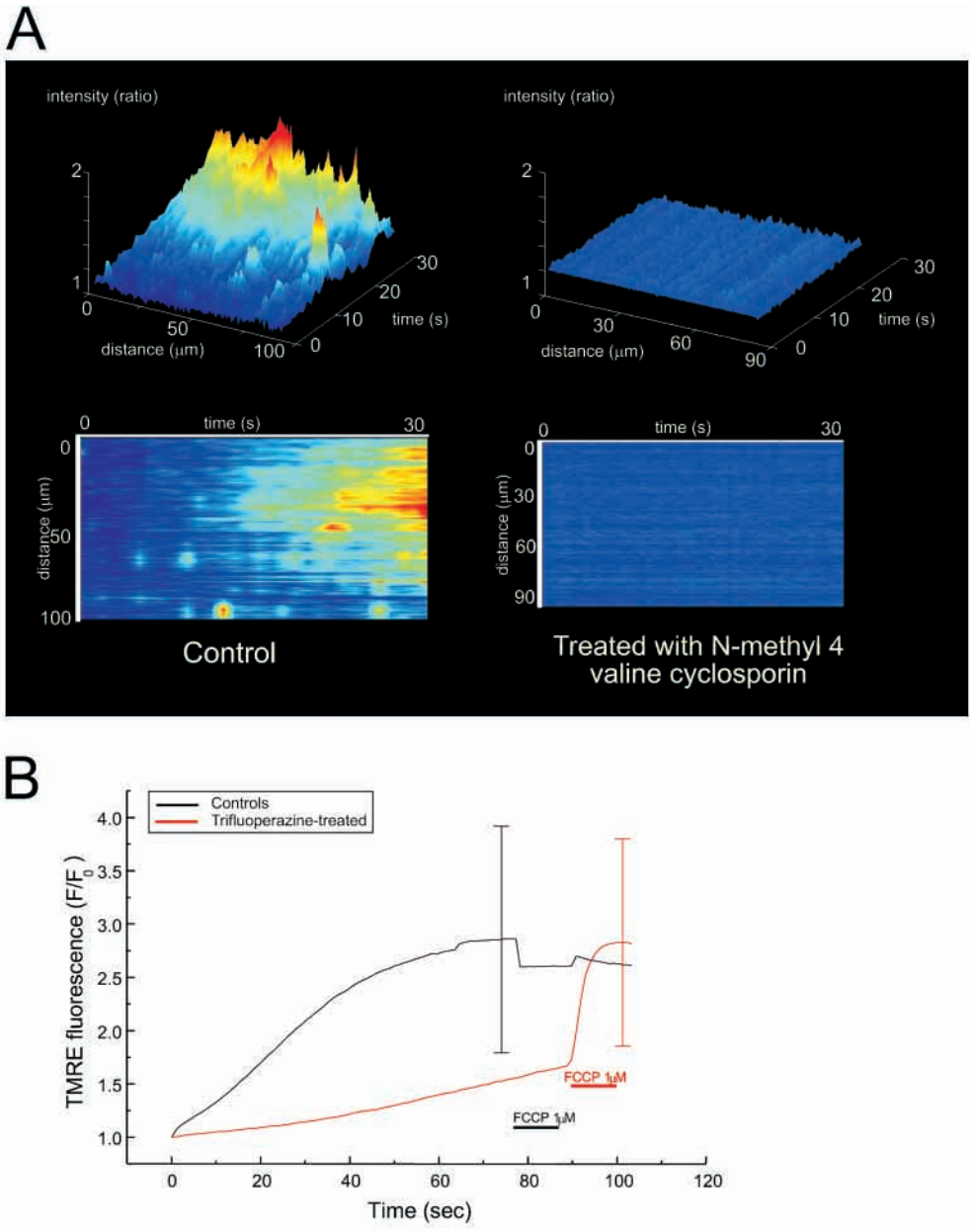

Fig. 6. The depolarisations reflected transient openings of the mitochondrial permeability transition pore. (A) Treatment of cells with N-methyl 4-valine cyclosporin (400 nM) reduced the incidence of transient depolarisations. Line images illustrate that mitochondrial flickering was almost completely prevented in cells treated with meth-v-Cs, which reduced the integrated activity from control values of 12.0±2.6 (n=122) to 9.8±2.5 (n=82) (mean±s.d., P<0.0001, two-tailed, unpaired t test), suggesting that the transient depolarisations were transient openings of the mPTP. (B) 10 μM Trifluoperazine, another inhibitor of mPTP formation, slowed the rate of global mitochondrial depolarisation, reducing the slope from a control of 0.041±0.018 (n=27 cells) to 0.008±0.006 (n=60 cells; P<0.0001).

were identified in the control group and only one was seen in the imaged group. Exposure of the astrocytes to 500 μM staurosporine revealed that the majority of treated cells were apoptotic after 4 hours, as defined by morphology and Hoechst staining (data not shown).

Discussion

Our data strongly suggest a mechanism that can account for the progression to cell death during pathological states involving increased mitochondrial ROS production. The increased generation of ROS within mitochondria initiates a sequence of events in which the oxidative stress increases the probability of Ca^{2+} release from ER. The very close proximity of ER and mitochondria (suggested by the failure of BAPTA to influence events) means that Ca^{2+} is accumulated by nearby mitochondria, further sensitising the mitochondria to the ROS, which then causes the mPTP to open. The mPTP openings are initially restricted to individual mitochondria, and are transient and reversible, but ultimately progress to the collapse of mitochondrial potential in the whole mitochondrial population. Remarkably, the transient 'flickering' mitochondrial depolarisations appear quite innocuous and have no apparent long-term consequence for cell fate, whereas the cells progress to necrotic cell death once the pore has opened fully.

Mitochondria and free radicals

Although 95-98% of the molecular oxygen that is consumed by mitochondria is reduced to water, the remainder is partially reduced by the addition of an electron, forming the oxyradical superoxide (Chance et al., 1979). Although mitochondrial antioxidant defences are extensive, excess mitochondrial ROS production or depletion of antioxidant defences cause oxidative

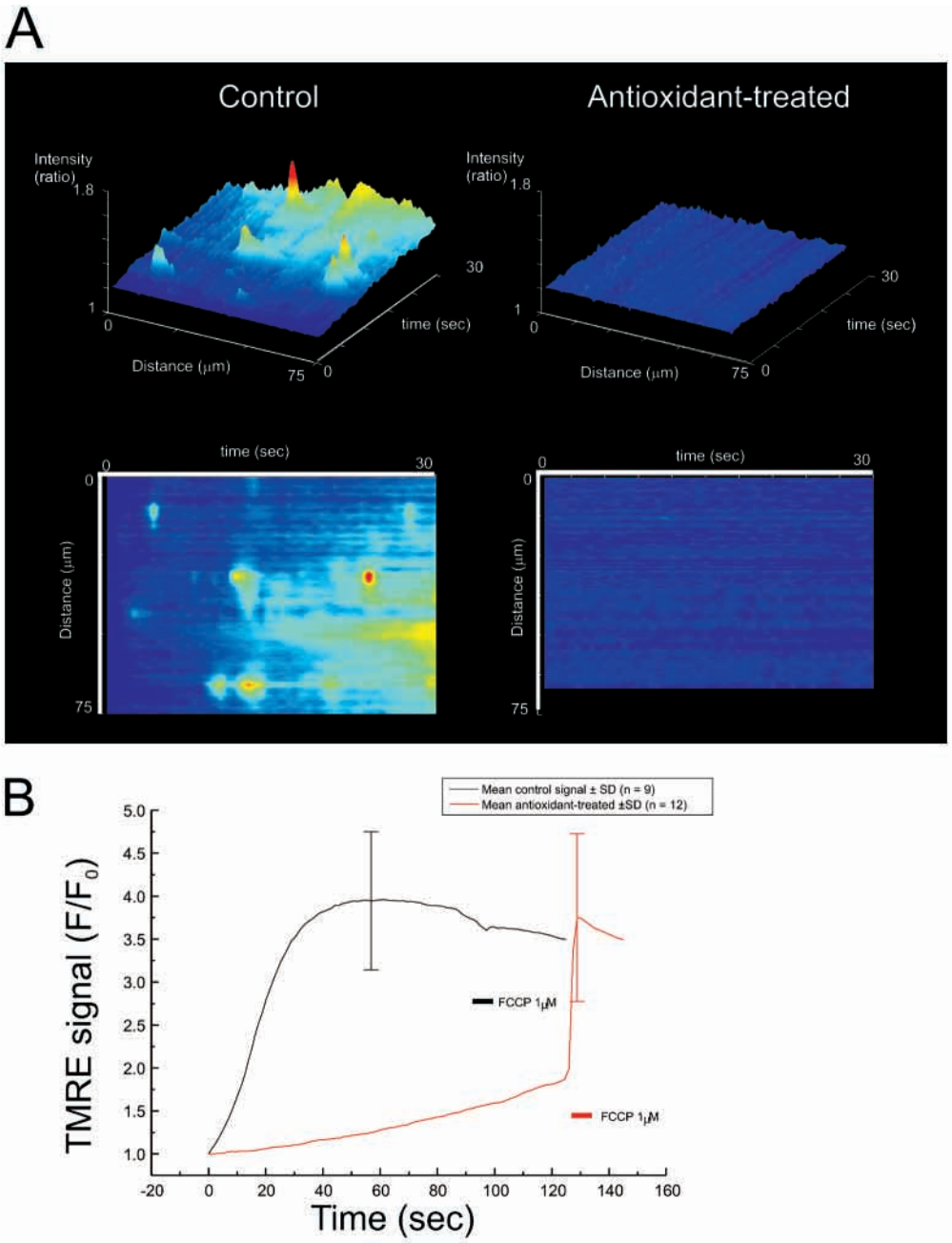

Fig. 7. Mitochondrial ROS are required for pore opening. (A) Treatment of cells with an array of antioxidants (1mM ascorbic acid, 250 units/ml catalase, 1mM Trolox and 500 μM of the spin trap TEMPO) reduced the incidence of mitochondrial depolarisations, reducing the integrated activity from a control of 10.0±5.6 (n=53 cells) to 6.4±1.9 (n=57) (P<0.001, Mann-Whitney U test). (B) The antioxidants also significantly increased the time to global mitochondrial depolarisation (P<0.0001, Mann-Whitney U test).

stress and, ultimately, cellular dysfunction. Indeed, mitochondrial ROS production may be a major mechanism of cell injury following anoxia and reperfusion. Many fluorophores generate ROS upon illumination (Bunting, 1992) and the consequent photosensitization causes apoptotic cell death in some cell lines (Minamikawa et al., 1999). Indeed, this is probably the basis for cell killing by sensitisers used in photodynamic therapy for some cancers (Fuchs and Thiele, 1998). ROS production by illuminated TMRE is specifically intramitochondrial, reflecting the mitochondrial localisation of the dye, and so this approach provides a useful model with which to generate a specific mitochondrial oxidative stress.

These data do not simply reflect the random toxicity of a fluorescent dye. The model of oxidative stress presented here deliberately uses two key properties of the potentiometric probe, TMRE. First, the well-described production of ROS upon illumination of TMRE provides a source of ROS (principally singlet oxygen) (Bunting, 1992) that varies with the intensity of illumination. Thus the oxidative stress may be ‘tuned’ by varying the incident excitation light. Second, the selective partitioning of TMRE into mitochondria means that the ROS are generated specifically from within the mitochondria. This therefore provides a controlled model of specific mitochondrial oxidative stress, perhaps the most appropriate model to study the metabolic oxidative stress seen for example in reperfusion injury. Oxidative stress that results from the exogenous application of pro-oxidants such as tert-butyl hydroperoxide or UV light may be significantly different because the immediate target of such treatments is likely to be the plasma membrane. The model presented here may be most

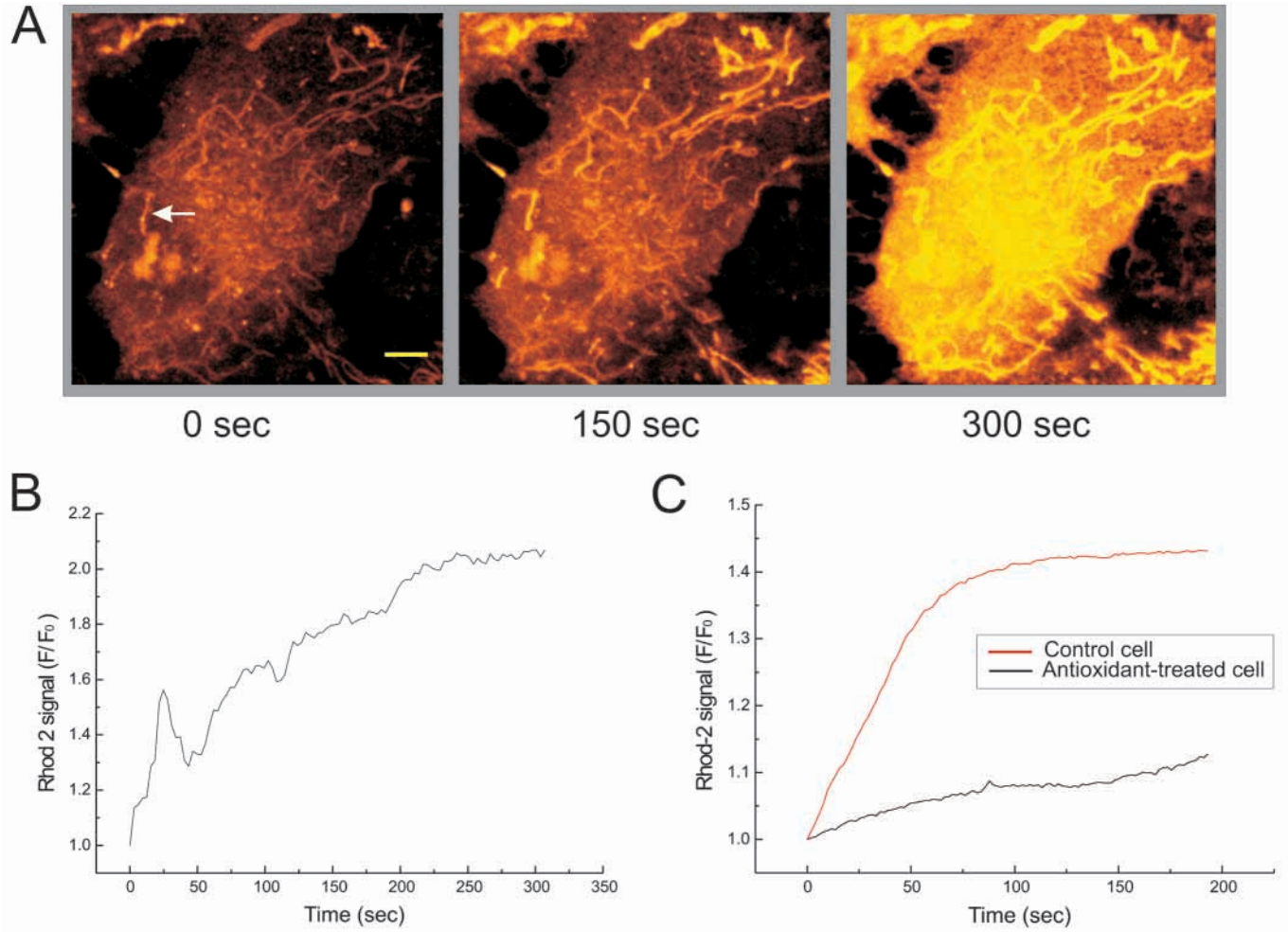

Fig. 8. Illumination of rhod-2 loaded astrocytes caused mitochondrial Ca^{2+}-loading. (A) Confocal images of an astrocyte loaded with the Ca^{2+}-indicator rhod-2. During illumination, the rhod-2 signal over the whole cell rose, including that over mitochondria. Excitation of the dye was elicited using the 543 nm line of a HeNe laser set to 4% of total output. The images were taken using a ×63 oil immersion lens; bar, 5 μm. The time course of rhod-2 signal change over a single mitochondrion is shown in B, which illustrates the signal measured over the mitochondrion marked by an arrow in A. Addition of antioxidants significantly reduced the rate of rise of rhod-2 signal (C), suggesting a role for ROS in the mitochondrial Ca^{2+}-loading.

instructive in understanding the pathophyisiology of the mitochondrial oxidative stress, implicated in ischaemia reperfusion (Halestrap et al., 1998), neurodegenerative disorders (Beal et al., 1997) and sepsis (Kantrow and Piantadosi, 1997).

The mitochondrial permeability transition pore

The opening of a high conductance mitochondrial pathway by a combination of high $[Ca^{2+}]_{mit}$, high inorganic phosphate and adenine nucleotide depletion has been recognised for many years (Hunter and Haworth, 1979). The pathway is now thought to reflect formation of a membrane-spanning proteinaceous pore, the mPTP, comprising (at least) the voltage dependent anion channel (VDAC), the adenine nucleotide translocase (ANT) and the mitochondrial cyclophilin D (Cyp D). Opening of the mPTP results in rapid dissipation of $\Delta\psi_m$, cessation of ATP synthesis, and mitochondrial swelling (Crompton et al., 1987; Halestrap et al., 1997; Hunter and Haworth, 1979; Zoratti and Szabó, 1994). Comprehensive investigation of isolated organelles has established a range of inducers and inhibitors of pore opening (for a review, see Zoratti and Szabò, 1995). Classic inducers of mPTP opening include mitochondrial Ca^{2+}-overload (Crompton and Costi, 1988), oxidative stress (Byrne et al., 1999; Nieminen et al., 1995) and depletion of adenine nucleotides (Crompton and Costi, 1990; Novgorodov et al., 1991), whereas the decapeptide cyclosporin A and related compounds, and agents that block the ANT reduce the probability of pore opening (Crompton et al., 1988; Halestrap and Davidson, 1990).

Extrapolating data acquired from isolated mitochondria to the complexity of the intact cell is not straightforward, although elegant models have been devised by using the redistribution of calcein into (Nieminen et al., 1995) and out of (Petronilli et al., 1998) mitochondria, to reveal openings of the pore. Mitochondrial Ca^{2+}-loading is essential for mPTP opening in isolated mitochondria, but intracellular mitochondrial Ca^{2+} uptake may depend upon a variety of

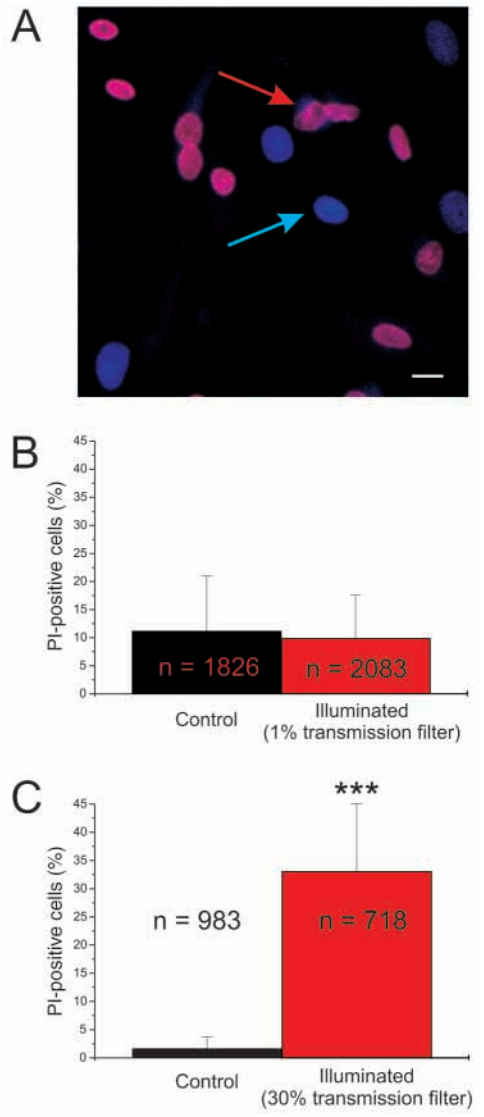

Fig. 9. Transient openings of the mPTP were innocuous: prolonged openings caused necrotic cell death. TMRE loaded cells were imaged using either a 1% neutral density filter, sufficient to image reversible mPTP openings, or a 30% filter, to induce global mitochondrial depolarisation. After a period of imaging, cells were returned to the incubator for 4 hours. They were then exposed to propidium iodide (PI) and Hoechst 33342 (A) in order to identify necrotic or apoptotic nuclei. PI stains damaged or necrotic cells (red arrow). Hoechst stains all nuclei (blue arrow), but apoptotic nuclei display a characteristic bright, condensed staining (not shown). Bar, 10 μm. Transient openings of the mPTP caused no increase in cell death, either by apoptosis or necrosis (B); however, global and complete mitochondrial depolarisation caused a significant increase in necrotic staining (P=0.0002). No sign of apoptotic morphology or Hoechst staining was apparent.

factors including ER-mitochondrial architecture (Rizzuto et al., 1993; Rizzuto et al., 1998), local redox state (Byrne et al., 1999; Jornot et al., 1999) and $\Delta\psi_m$ (Nicholls and Crompton, 1980). Although it is clear that oxidative stress sensitises isolated mitochondria to Ca^{2+} and mPTP opening (Petronilli et al., 1994a; Valle et al., 1993), ROS may have a range of molecular targets, including mitochondrial membrane lipids (Nomura et al., 1999) and the respiratory chain complexes (Heales et al., 1995).

Mitochondrially generated ROS causes mitochondrial Ca^{2+}-loading from ER stores

It is clear that mPTP opening in isolated mitochondria requires Ca^{2+}-loading (Crompton et al., 1987). Similarly, in models of oxidative stress, mitochondrial Ca^{2+}-loading was necessary for pore formation (Byrne et al., 1999). Our present data strongly suggest that the source of that Ca^{2+} is the ER: the transient openings of the mPTP and the global depolarisation were both independent of external Ca^{2+}, but were dramatically attenuated by emptying ER Ca^{2+} stores and chelating Ca^{2+}. Furthermore, mitochondrial Ca^{2+} loading by illumination was demonstrable, dependent on ER Ca^{2+} stores and inhibited by antioxidants. The fact that neither ER Ca^{2+} depletion nor Ca^{2+} chelation was sufficient alone but that both together stopped mitochondrial Ca^{2+}-loading and inhibited mPTP opening strongly argues that ER and mitochondria must be closely apposed in these cells, as described for HeLa cells (Rizzuto et al., 1998), RBL-2H3 cells (Csordas et al., 1999) and cardiomyocytes (Ramesh et al., 1998). The impact of mitochondrial Ca^{2+} uptake on the rate of propagation of calcium waves in astrocytes would also support this proposition (Boitier et al., 1999). These data add further to a body of literature suggesting the expression of a privileged pathway of ER Ca^{2+}-release and mitochondrial Ca^{2+}-uptake at least in some cell types. It is also interesting that several recent reports have emphasised the organisation of mitochondria as a contiguous network (e.g. Rutter and Rizzuto, 2000). In astrocytes, confocal imaging allows individual mitochondrial structures to be seen clearly, and the mitochondrial depolarisations were evidently independent in time and space, suggesting that here the mitochondrial organisation is more complex.

A substantial literature suggests that ROS may modulate the gating of ryanodine-sensitive Ca^{2+} channels in the SR (Boraso and Williams, 1994; Holmberg and Williams, 1992) probably through modification of critical thiol groups (Kourie, 1998). Data that indicate modulation of Ins(1,4,5)P_3-mediated Ca^{2+} channels by ROS are less abundant. Oxidised glutathione (Henschke and Elliott, 1995) and ROS derived from xanthine/xanthine oxidase (Wesson and Elliott, 1995) have been shown to induce Ca^{2+}-release from Ins(1,4,5)P_3-mediated stores in endothelial cells and superoxide may stimulate Ins(1,4,5)P_3-mediated Ca^{2+} release in vascular smooth muscle cells (Suzuki and Ford, 1992). As the opening of the mPTP is also regulated by thiols (Kowaltowski et al., 1998), it seems that the sensitivity of both the Ins(1,4,5)P_3 receptor and the mPTP to redox state renders this whole system susceptible to oxidative damage through the initiation of a destructive feedback cycle, whereby increased mitochondrial ROS production increases the local probability of ER Ca^{2+} release and mitochondrial Ca^{2+} loading. This may both increase ROS generation further (Dykens, 1994) and sensitise the mitochondria to ROS, culminating in mPTP opening, initially in a transient and reversible mode and later in a global irreversible mode. We have then asked what the implications of mPTP opening in these different states are for cell fate.

Flickering openings of the mPTP were innocuous but sustained pore opening induced necrotic death

Studies of the mPTP in isolated mitochondria showed that the pore may flicker before opening fully, and the existence of sub-conductance states has been suggested (Zoratti and Szabó, 1994). Recently, transient opening of the mPTP has been suggested to underlie initiation of apoptosis in single hepatocytes (Szalai et al., 1999), but it is unclear whether these were reversible openings of the pore in full or flickering openings of a sub-conductance state. Opening of the mPTP is expected to have catastrophic consequences for cell fate. As the driving force of the ATP-synthase is the mitochondrial potential, complete dissipation of the $\Delta\psi_m$ can cause reversal of the ATP synthase, which now consumes ATP while pumping protons from the mitochondrial matrix. Rapid consumption of cellular ATP may in turn lead to energetic collapse and necrotic cell death (Leyssens et al., 1996). Additionally, cytochrome c may be released from the mitochondrial intermembrane space, possibly after mitochondrial swelling and outer membrane disruption, activating the caspase cascade and initiating apoptotic cell death (Liu et al., 1996). Opening of the mPTP may also release apoptosis-inducing factor (AIF), a soluble protein that activates caspase 3 (Susin et al., 1997). Therefore, opening of the mPTP may predict either necrotic or apoptotic cell death.

Using our model of mitochondrial oxidative stress and mPTP opening we found that single mitochondria may undergo repeated, transient openings of the pore that seem to have no deleterious effect on cell function. Among those cells in which pore openings were transient and reversible, there was no evidence of either necrotic or apoptotic cell death at 4 hours. However, sustained mPTP opening clearly increased the incidence of necrotic cell death. It seems likely that, in primary cells, where oxidative phosphorylation is the dominant source of intracellular ATP, mPTP opening will cause rapid ATP consumption and therefore predict a necrotic death.

We thank D. Lilian Patterson for expert technical assistance and cell culture. Some of the work shown was conducted as part of a final year undergraduate BSc program by Nkechi Ebele, Sashini Perera and Tahir Mahmud, whom we thank for their hard work. We also thank the Medical Research Council for financial support.

References

Beal, M. F., Howell, N. and Bodis-Wollner, I. (1997). *Mitochondria and Free Radicals in Neurodegenerative Disease*. New York: Wiley-Liss.

Bernardi, P., Veronese, P. and Petronilli, V. (1993). Modulation of the mitochondrial cyclosporin A-sensitive permeability transition pore. I. Evidence for two separate Me^{2+} binding sites with opposing effects on the pore open probability. *J. Biol. Chem.* **268**, 1005-1010.

Bernardi, P., Scorrano, L., Colonna, R., Petronilli, V. and Di Lisa, F. (1999). Mitochondria and cell death. Mechanistic aspects and methodological issues. *Eur. J. Biochem.* **264**, 687-701.

Boitier, E., Rea, R. and Duchen, M. R. (1999). Mitochondria exert a negative feedback on the propagation of intracellular Ca^{2+} waves in rat cortical astrocytes. *J. Cell Biol.* **145**, 795-808.

Boraso, A. and Williams, A. J. (1994). Modification of the gating of the cardiac sarcoplasmic reticulum Ca^{2+}-release channel by H2O2 and dithiothreitol. *Am. J. Physiol.* **267**, H1010-H1016.

Buckman, J. F. and Reynolds, I. J. (2001). Spontaneous changes in mitochondrial membrane potential in cultured neurons. *J. Neurosci.* **21**, 5054-5065.

Bunting, J. R. (1992). A test of the singlet oxygen mechanism of cationic dye photosensitization of mitochondrial damage. *Photochem. Photobiol.* **55**, 81-87.

Bunting, J. R., Phan, T. V., Kamali, E. and Dowben, R. M. (1989). Fluorescent cationic probes of mitochondria. Metrics and mechanism of interaction. *Biophys. J.* **56**, 979-993.

Byrne, A. M., Lemasters, J. J. and Nieminen, A. L. (1999). Contribution of increased mitochondrial free Ca^{2+} to the mitochondrial permeability transition induced by tert-butylhydroperoxide in rat hepatocytes. *Hepatology* **29**, 1523-1531.

Chamberlain, B. K., Volpe, P. and Fleischer, S. (1984). Inhibition of calcium-induced calcium release from purified cardiac sarcoplasmic reticulum vesicles. *J. Biol. Chem.* **259**, 7547-7553.

Chance, B., Sies, H. and Boveris, A. (1979). Hydroperoxide metabolism in mammalian organs. *Physiol. Rev.* **59**, 527-605.

Crompton, M. (1999). The mitochondrial permeability transition pore and its role in cell death. *Biochem. J.* **341**, 233-249.

Crompton, M. and Costi, A. (1988). Kinetic evidence for a heart mitochondrial pore activated by Ca^{2+}, inorganic phosphate and oxidative stress. A potential mechanism for mitochondrial dysfunction during cellular Ca^{2+} overload. *Eur. J. Biochem.* **178**, 489-501.

Crompton, M. and Costi, A. (1990). A heart mitochondrial Ca^{2+}-dependent pore of possible relevance to re-perfusion-induced injury. Evidence that ADP facilitates pore interconversion between the closed and open states. *Biochem. J.* **266**, 33-39.

Crompton, M., Costi, A. and Hayat, L. (1987). Evidence for the presence of a reversible Ca^{2+}-dependent pore activated by oxidative stress in heart mitochondria [published erratum appears in *Biochem. J.* 1987, 246, following 806]. *Biochem. J.* **245**, 915-918.

Crompton, M., Ellinger, H. and Costi, A. (1988). Inhibition by cyclosporin A of a Ca^{2+}-dependent pore in heart mitochondria activated by inorganic phosphate and oxidative stress. *Biochem. J.* **255**, 357-360.

Csordas, G., Thomas, A. P. and Hajnoczky, G. (1999). Quasi-synaptic calcium signal transmission between endoplasmic reticulum and mitochondria. *EMBO J.* **18**, 96-108.

De Giorgi, F., Lartigue, L. and Ichas, F. (2000). Electrical coupling and plasticity of the mitochondrial network. *Cell Calcium* **28**, 365-370.

Duchen, M. R. (1992). Ca^{2+}-dependent changes in the mitochondrial energetics in single dissociated mouse sensory neurons. *Biochem. J.* **283**, 41-50.

Duchen, M. R. and Biscoe, T. J. (1992). Relative mitochondrial membrane potential and $[Ca^{2+}]i$ in type I cells isolated from the rabbit carotid body. *J. Physiol.* **450**, 33-61.

Duchen, M. R., Leyssens, A. and Crompton, M. (1998). Transient mitochondrial depolarizations reflect focal sarcoplasmic reticular calcium release in single rat cardiomyocytes. *J. Cell Biol.* **142**, 975-988.

Duranteau, J., Chandel, N. S., Kulisz, A., Shao, Z. and Schumacker, P. T. (1998). Intracellular signaling by reactive oxygen species during hypoxia in cardiomyocytes. *J. Biol. Chem.* **273**, 11619-11624.

Dykens, J. A. (1994). Isolated cerebral and cerebellar mitochondria produce free radicals when exposed to elevated Ca^{2+} and Na^{+}: implications for neurodegeneration. *J. Neurochem.* **63**, 584-591.

Fuchs, J. and Thiele, J. (1998). The role of oxygen in cutaneous photodynamic therapy. *Free Radic. Biol. Med.* **24**, 835-847.

Gutteridge, J. M. and Mitchell, J. (1999). Redox imbalance in the critically ill. *Br. Med. Bull.* **55**, 49-75.

Halestrap, A. P. and Davidson, A. M. (1990). Inhibition of Ca^{2+}-induced large-amplitude swelling of liver and heart mitochondria by cyclosporin is probably caused by the inhibitor binding to mitochondrial-matrix peptidyl-prolyl cis-trans isomerase and preventing it interacting with the adenine nucleotide translocase. *Biochem. J.* **268**, 153-160.

Halestrap, A. P., Woodfield, K. Y. and Connern, C. P. (1997). Oxidative stress, thiol reagents, and membrane potential modulate the mitochondrial permeability transition by affecting nucleotide binding to the adenine nucleotide translocase. *J. Biol. Chem.* **272**, 3346-3354.

Halestrap, A. P., Kerr, P. M., Javadov, S. and Woodfield, K. Y. (1998). Elucidating the molecular mechanism of the permeability transition pore and its role in reperfusion injury of the heart. *Biochim. Biophy. Acta* **1366**, 79-94.

Halliwell, B. and Gutteridge, J. M. C. (1998). *Free Radicals in Biology and Medicine*. Oxford: Oxford University Press.

Heales, S. J., Davies, S. E., Bates, T. E. and Clark, J. B. (1995). Depletion of brain glutathione is accompanied by impaired mitochondrial function and decreased N-acetyl aspartate concentration. *Neurochem. Res.* **20**, 31-28.

Henschke, P. N. and Elliott, S. J. (1995). Oxidized glutathione decreases luminal Ca2+ content of the endothelial cell ins(1,4,5)P3-sensitive Ca^{2+} store. *Biochem. J.* **312**, 485-489.

Holmberg, S. R. and Williams, A. J. (1992). The calcium-release channel from cardiac sarcoplasmic reticulum: function in the failing and acutely ischaemic heart. *Basic Res. Cardiol.* **87**, 255-268.

Hunter, D. R. and Haworth, R. A. (1979). The Ca^{2+}-induced membrane transition in mitochondria. I. The protective mechanisms. *Arch. Biochem. Biophys.* **195**, 453-459.

Hüser, J., Rechenmacher, C. E. and Blatter, L. A. (1998). Imaging the permeability pore transition in single mitochondria. *Biophys. J.* **74**, 2129-2137.

Jacobson, D. and Duchen, M. R. (1998). Fluorescence imaging of the mitochondrial permeability transition in rat cortical astrocytes in culture. *J. Physiol.* **506.P**, 75P.

Jornot, L., Maechler, P., Wollheim, C. B. and Junod, A. F. (1999). Reactive oxygen metabolites increase mitochondrial calcium in endothelial cells: implication of the Ca^{2+}/Na^{+} exchanger. *J. Cell Sci.* **112**, 1013-1022.

Kantrow, S. P. and Piantadosi, C. A. (1997). Release of cytochrome c from liver mitochondria during permeability transition. *Biochem. Biophys. Res. Commun.* **232**, 669-671.

Kourie, J. I. (1998). Interaction of reactive oxygen species with ion transport mechanisms. *Am. J. Physiol.* **275**, C1-C24.

Kowaltowski, A. J., Netto, L. E. and Vercesi, A. E. (1998). The thiol-specific antioxidant enzyme prevents mitochondrial permeability transition. Evidence for the participation of reactive oxygen species in this mechanism. *J. Biol. Chem.* **273**, 12766-12769.

Kroemer, G. (1999). Mitochondrial control of apoptosis: an overview. In *Mitochondria and Cell Death* (ed. G. C. Brown, D. G. Nicholls and C. E. Cooper), pp. 1-15. London: Portland Press.

Langley, D. and Pearce, B. (1994). Ryanodine-induced intracellular calcium mobilisation in cultured astrocytes. *Glia* **12**, 128-134.

Lemasters, J. J., Nieminen, A. L., Qian, T., Trost, L. C., Elmore, S. P., Nishimura, Y., Crowe, R. A., Cascio, W. E., Bradham, C. A., Brenner, D. A. et al. (1998). The mitochondrial permeability transition in cell death: a common mechanism in necrosis, apoptosis and autophagy. *Biochim. Biophys. Acta* **1366**, 177-196.

Lenaz, G. (1998). Role of mitochondria in oxidative stress and ageing. *Biochim. Biophys. Acta* **1366**, 53-67.

Leyssens, A., Anderson, M., Craske, M., Ratoghi, R., Crompton, M. and Duchen, M. R. (1995). Transient depolarisations of mitochondria localised to discrete areas of single rat cardiomyocytes caused by free radicals and local calcium release: a model for free radical induced cell injury. *J. Physiol.* **487P**, 123P.

Leyssens, A., Nowicky, A. V., Patterson, L., Crompton, M. and Duchen, M. R. (1996). The relationship between mitochondrial state, ATP hydrolysis, [Mg2+]i and [Ca2+]i studied in isolated rat cardiomyocytes. *J. Physiol.* **496**, 111-128.

Liu, X., Kim, C. N., Yang, J., Jemmerson, R. and Wang, X. (1996). Induction of apoptotic program in cell-free extracts: requirement for dATP and cytochrome c. *Cell* **86**, 147-157.

Matlib, M. A., Zhou, Z., Knight, S., Ahmed, S., Choi, K. M., Krause-Bauer, J., Phillips, R., Altschuld, R., Katsube, Y., Sperelakis, N. et al. (1998). Oxygen-bridged dinuclear ruthenium amine complex specifically inhibits Ca^{2+} uptake into mitochondria in vitro and in situ in single cardiac myocytes. *J. Biol. Chem.* **273**, 10223-10231.

Minamikawa, T., Sriratana, A., Williams, D. A., Bowser, D. N., Hill, J. S. and Nagley, P. (1999). Chloromethyl-X-rosamine (MitoTracker Red) photosensitises mitochondria and induces apoptosis in intact human cells. *J. Cell Sci.* **112**, 2419-2430.

Nicholls, D. G. and Crompton, M. (1980). Mitochondrial calcium transport. *FEBS Lett.* **111**, 261-268.

Nicholls, D. G. and Ward, M. W. (2000). Mitochondrial membrane potential and neuronal glutamate excitotoxicity: mortality and millivolts. *Trends Neurosci.* **23**, 166-174.

Nieminen, A. L., Saylor, A. K., Tesfai, S. A., Herman, B. and Lemasters, J. J. (1995). Contribution of the mitochondrial permeability transition to lethal injury after exposure of hepatocytes to t-butylhydroperoxide. *Biochem. J.* **307**, 99-106.

Nomura, K., Imai, H., Koumura, T., Arai, M. and Nakagawa, Y. (1999). Mitochondrial phospholipid hydroperoxide glutathione peroxidase suppresses apoptosis mediated by a mitochondrial death pathway. *J. Biol. Chem.* **274**, 29294-29302.

Novgorodov, S. A., Gudz, T. I., Jung, D. W. and Brierley, G. P. (1991). The nonspecific inner membrane pore of liver mitochondria: modulation of cyclosporin sensitivity by ADP at carboxyatractyloside-sensitive and insensitive sites. *Biochem. Biophys. Res. Commun.* **180**, 33-38.

Petronilli, V., Costantini, P., Scorrano, L., Colonna, R., Passamonti, S. and Bernardi, P. (1994a). The voltage sensor of the mitochondrial permeability transition pore is tuned by the oxidation-reduction state of vicinal thiols. Increase of the gating potential by oxidants and its reversal by reducing agents. *J. Biol. Chem.* **269**, 16638-16642.

Petronilli, V., Nicolli, A., Costantini, P., Colonna, R. and Bernardi, P. (1994b). Regulation of the permeability transition pore, a voltage-dependent mitochondrial channel inhibited by cyclosporin A. *Biochim. Biophys. Acta* **1187**, 255-259.

Petronilli, V., Miotto, G., Canton, M., Colonna, R., Bernardi, P. and Di Lisa, F. (1998). Imaging the mitochondrial permeability transition pore in intact cells. *Biofactors* **8**, 263-272.

Peuchen, S., Clark, J. B. and Duchen, M. R. (1996). Mechanisms of intracellular calcium regulation in adult astrocytes. *Neuroscience* **71**, 871-883.

Peuchen, S., Bolaños, J. P., Heales, S. J., Almeida, A., Duchen, M. R. and Clark, J. B. (1997). Interrelationships between astrocyte function, oxidative stress and antioxidant status within the central nervous system. *Prog. Neurobiol.* **52**, 261-281.

Qian, T., Herman, B. and Lemasters, J. J. (1999). The mitochondrial permeability transition mediates both necrotic and apoptotic death of hepatocytes exposed to Br-A23187. *Toxicol. Appl. Pharmacol.* **154**, 117-125.

Ramesh, V., Sharma, V. K., Sheu, S. S. and Franzini-Armstrong, C. (1998). Structural proximity of mitochondria to calcium release units in rat ventricular myocardium may suggest a role in Ca^{2+} sequestration. *Ann. New York Acad. Sci.* **853**, 341-344.

Ricken, S., Leipziger, J., Greger, R. and Nitschke, R. (1998). Simultaneous measurements of cytosolic and mitochondrial Ca^{2+} transients in HT29 cells. *J. Biol. Chem.* **273**, 34961-34969.

Rizzuto, R., Brini, M., Murgia, M. and Pozzan, T. (1993). Microdomains with high Ca2+ close to IP3-sensitive channels that are sensed by neighboring mitochondria. *Science* **262**, 744-747.

Rizzuto, R., Pinton, P., Carrington, W., Fay, F. S., Fogarty, K. E., Lifshitz, L. M., Tuft, R. A. and Pozzan, T. (1998). Close contacts with the endoplasmic reticulum as determinants of mitochondrial Ca^{2+} responses. *Science* **280**, 1763-1766.

Rutter, G. A. and Rizzuto, R. (2000). Regulation of mitochondrial metabolism by ER Ca2+ release: an intimate connection. *Trends Biochem. Sci.* **25**, 215-221.

Sheu, S. S. and Sharma, V. K. (1999). Rapid report: a novel technique for quantitative measurement of free Ca^{2+} concentration in rat heart mitochondria. *J. Physiol.* **518**, 577-584.

Susin, S. A., Zamzami, N., Castedo, M., Daugas, E., Wang, H. G., Geley, S., Fassy, F., Reed, J. C. and Kroemer, G. (1997). The central executioner of apoptosis: multiple connections between protease activation and mitochondria in Fas/APO-1/CD95- and ceramide-induced apoptosis. *J. Exp. Med.* **186**, 25-37.

Suzuki, Y. J. and Ford, G. D. (1992). Superoxide stimulates IP3-induced Ca^{2+} release from vascular smooth muscle sarcoplasmic reticulum. *Am. J. Physiol.* **262**, H114-H116.

Szalai, G., Krishnamurthy, R. and Hajnoczky, G. (1999). Apoptosis driven by IP3-linked mitochondrial calcium signals. *EMBO J.* **18**, 6349-6361.

Turrens, J. F. and Boveris, A. (1980). Generation of superoxide anion by the NADH dehydrogenase of bovine heart mitochondria. *Biochem. J.* **191**, 421-427.

Valle, V. G., Fagian, M. M., Parentoni, L. S., Meinicke, A. R. and Vercesi, A. E. (1993). The participation of reactive oxygen species and protein thiols in the mechanism of mitochondrial inner membrane permeabilization by calcium plus prooxidants. *Arch. Biochem. Biophys.* **307**, 1-7.

Wesson, D. E. and Elliott, S. J. (1995). The H2O2-generating enzyme, xanthine oxidase, decreases luminal Ca^{2+} content of the IP3-sensitive Ca^{2+} store in vascular endothelial cells. *Microcirculation* **2**, 195-203.

Zoratti, M. and Szabó, I. (1994). Electrophysiology of the inner mitochondrial membrane. *J. Bioenerg. Biomembr.* **26**, 543-553.

Zoratti, M. and Szabò, I. (1995). The mitochondrial permeability transition. *Biochim. Biophys. Acta* **1241**, 139-176.

Zorov, D. B., Filburn, C. R., Klotz, L. O., Zweier, J. L. and Sollott, S. J. (2000). Reactive oxygen species (ROS)-induced ROS release: a new phenomenon accompanying induction of the mitochondrial permeability transition in cardiac myocytes. *J. Exp. Med.***192**, 1001-1014.